ARID ZONE JOURNAL OF ENGINEERING, TECHNOLOGY & ENVIRONMENT
AZOJETE June 2025. Vol.21(2):545-556
Published by the Faculty of Engineering, University of Maiduguri, Maiduguri, Nigeria.
Print ISSN: 1596-2490, Electronic ISSN: 2545-5818
https://doi.org/10.63958/AZOJETE/2025/21/02/019
www.azojete.com.ng

ORIGINAL RESEARCH ARTICLE

TILAPIA FISH SCALE-DERIVED HYDROXYAPATITE INHIBITOR FOR COPPER CORROSION: ELECTROCHEMICAL, ADSORPTION, AND MECHANISTIC INVESTIGATIONS

O. S. I. Fayomi[1,2*]

[1]Department of Mechanical Engineering, Bells University of Technology, Ogun State, Nigeria
[2]Department of Mechanical Engineering Science, University of Johannesburg, Johannesburg, South Africa
[*]Corresponding author's email: ojosundayfayomi3@gmail.com, osfayomi@bellsuniversity.edu.ng

ARTICLE INFORMATION

Received: 24th April 2025
Revised: 1st May 2025
Accepted: 2nd May 2025

Keywords:
Copper
Corrosion
Inhibition
Optimization
Fish scale
Hydroxyapatite

ABSTRACT

This investigation analyzes hydroxyapatite (HAp) derived from tilapia fish scales as a green and sustainable corrosion inhibitor for copper in 1M HCl. While fish scales are an abundant biowaste source, the use of the scales' in assessing its corrosion inhibition capability will provide an eco-compatible option for the protection of industrial metals. The hydroxyapatite was purified using a multi-step process consisting of deproteinization, alkaline treatment, and high-temperature calcination under 1000°C to yield a purified nano-HAp powder. Open Circuit Potential (OCP), Linear Sweep Voltammetry (LSV), and Tafel polarization were used to determine the corrosion inhibition efficiency under various temperatures (30°C, 40°C, and 50°C) and different concentrations (0.2 g, 0.4 g, and 0.6 g). The results showed an extensive reduction in the current density of the corrosion and the rate of the corrosion, with a maximum inhibition efficiency of (~95%) occurring under the 0.6 g concentration. The analysis of the adsorption showed that the inhibitor conformed to the Freundlich and Temkin isotherms, inferring multilayer adsorption and strong surface interactions. Optical micrographs corroborated the protective capability of the inhibitor through reduced roughness of the surface and reduced pitting. This study established that hydroxyapatite obtained from fish scales is an effective alternative, and eco-compatible corrosion inhibitor, contributing to waste reduction and green chemistry.

1.0 Introduction

Corrosion is an electrochemical process in nature that drives the metal back to its original state. This phenomenon occurs in the presence of a reactive environment, which facilitates the formation of an electrochemical cell (Abod *et al.,* 2019). Corrosion can also not only facilitate economic losses but lead to many health and safety hazards. Therefore, providing effective protection of metals is essential for the safety of people (Li *et al.,* 2021). Over the years, a variety of methods for the control of corrosion in metals have been established, but the use of inhibitors is still one of the best methods of protecting metals against corrosion (Arthur *et al.,* 2013; Wang *et al.,* 2007). However, conventional corrosion control methods frequently involve toxic, hazardous, and ecologically harmful inhibitors that pose serious risks to human health and the environment (Kadhim *et al.,* 2021; Ezzat *et al.,* 2022). In response, recent research has increasingly focused on developing sustainable corrosion inhibitors that offer both high efficiency and environmental compatibility (Kadhim *et al.,* 2021; Ezzat *et al.,* 2022; Aydinsoy *et al.,* 2024).

Biowaste obtained from fish, especially fish scales continuously constitute a plethora of health and environmental hazards since they are usually disposed in open spaces, particularly in coastal areas (Panda, Pramanik, & Sukla, 2014). A study estimate that the global processing of aquatic products generates an average of approximately 67 million tonnes annually (Tacon, 2020). Of this total, waste materials account for a significant portion, with fish scales alone representing about 5% of the discarded waste (Coppola *et al.,* 2021). This equates to over 30% of the overall volume of aquatic products processed (Duan *et al.,* 2004). Hence, fish-based industries and markets waste face a dilemma in the disposal of associated wastes (Zainol *et al.,* 2019).

Tilapia fish scales consist of approximately 40% to 55% organic components, including collagen, lipids, proteins, and vitamins, along with around 30% inorganic substances such as calcium and phosphates, making them a valuable biomaterial (Chinh *et al.,* 2019).

Calcium hydroxyphosphate, commonly known as hydroxyapatite, is represented by the chemical formula $Ca_5(PO_4)_3(OH)$ (Zhao *et al.,* 2025), although, it is more frequently expressed in its expanded form as $Ca_{10}(PO_4)_6(OH)_2$. This compound can be obtained from various natural waste materials, including fish scales, eggshells, and crab shells, which serve as sustainable and eco-friendly sources for its production (Abudullah *et al.,* 2020). These materials, are often considered as wastes, offer a valuable opportunity for resource recovery and utilization in the creation of hydroxyapatite (Sockalingam & Abdullah, 2015). Hydroxyapatite (Hap), is currently employed as a biosorbent in wastewater treatment (Selimin *et al.,* 2022), and as a biomedical material for bone repair and dental implants (DileepKumar *et al.,* 2022), among various other applications. As an inhibitor, Nyambi *et al.,* (2024) studied the physicochemical characterisation and computational studies of Tilapia fish scales as a green inhibitor for steel corrosion. The XRD analysis revealed the presence of a significant quantity of hydroxyapatite, as indicated by a prominent diffraction peak at $2\theta \approx 32°$. Additionally, amorphous collagen was inferred indirectly through a broad hump in the baseline within the 2θ range of 13°–25°. Both experimental and computational studies demonstrated that Tilapia fish scales can serve as an effective green corrosion inhibitor. This is attributed to the presence of key components such as collagen, hydroxyapatite, and various amino acids within the scales (Nyambi *et al.,* 2024). However, there is no available literature on the application of Tilapia fish scales as a corrosion inhibitor. This study thus seeks to investigate Tilapia fish scale-derived hydroxyapatite as an inhibitor for copper corrosion.

2. Materials and Method

2.1 Hydroxyapatite Powder Preparation from Tilapia Fish Scales

The tilapia scales were collected from a local fish market in Ota, Ogun State. They were first soaked in tap water, and then washed several times with distilled water to remove all the blood, dirt, and any other impurities before being left to dry. The scales were then deproteinized by washing them with 0.1M HCl. Afterwards, they were washed again with distilled water and put in the laboratory oven at 60°C for 45 minutes. The dry fish scales were ground to powder in a mechanical grinder. To treat the powder-like fish scales, 5M NaOH was poured into the powder and heated to a high temperature of 100°C, after which the sludge-like resulting mixture was stirred for an hour. The resulting treated powder was then washed thoroughly until the washing solution became neutral. It was poured through a filter paper, with the filtrate dried in a laboratory oven for 80°C. The resultant powder was subjected to calcination at 1000°C for 2 hours and 30 minutes to eliminate organic compounds and yield pure nano-HAp, in accordance with the methodology described by Zainol *et al.* (2019).

2.2 Other Materials Preparation

Prior to conducting electrochemical measurements, a 1 cm^2 section of a 99.99% pure copper sample was prepared and characterized as shown in Table 1. The surface was sequentially polished using sandpaper with grit sizes of 400, 800, 1200, and 2000. After the polishing, the smooth electrode was thoroughly rinsed in double-distilled water to remove any residues. Finally, it was dried using a dryer at room temperature. The 1M HCl solution was obtained from the in-house chemistry laboratory.

Table 1: Chemical compositional makeup of Copper Sample

Element	M (mass%) $\times 10^{-3}$
Si	7
P	16.5
Ti	0.4
V	0.3
Mn	2.65
Sb	0.6
Co	0.15
Ni	2.8
Nb	1.6
Mo	1.1
Sn	2.7
Cu	Bal.

Corresponding author's email address: ojosundayfayomi3@gmail.com, osfayomi@bellsuniversity.edu.ng

2.3 Electrochemical Measurements

A standard three-electrode system was used in conducting the electrochemical tests. The setup included a CS100 Potentiostat, operated by CS Studio6 and CS Analysis software. The three-electrode system was placed in a 100 mL beaker, which was then positioned in a water bath to maintain consistent temperatures of 30°C, 40°C, and 50°C throughout the experiment. Electrochemical measurements were performed using varying concentrations of hydroxyapatite (HAp): 0g (control test without inhibitor), 0.2g, 0.4g, and 0.6g of the inhibitor, each dissolved in 50 mL of 1M HCl solution as shown in Table 2. Polarization measurements were recorded at a scan rate of 0.01 V/s, covering a potential range from -1.5 V to +1.5 V. A similar methodology was carried out by Kehinde *et al.,* (2025).

Table 2: Experimental Arrangement

Experimental Arrangement	Test environment
Control	50ml HCl
0.2g HAp	0.2g HAp + 50ml HCl
0.4g HAp	0.4g HAp+ 50ml HCl
0.3g HAp	0.6g HAp + 50ml HCl

2.4 Adsorption and Mechanistic Studies

Key electrochemical parameters, including surface coverage, corrosion current density (J_{corr}), corrosion potential (E_{corr}), and inhibition efficiency (IE%), were determined using Tafel plots and Equations 1 and 2. Additionally, the adsorption behaviour of the HAp was analysed using adsorption models, specifically the Langmuir, Freundlich, and Temkin isotherms. Statistical analysis for the experiments was also included using Design Expert Software 13 at a 95% confidence level. Mathematical regression models and Response Surface Methodology (RSM) were further used to evaluate and predict the inhibitor's performance. Analysis of variance (ANOVA) was utilized in assessing the influence of process variables on the corrosion rate response, providing critical insights for process optimization.

$$\text{Surface Coverage } (\theta) = \frac{j^0corr - jcorr}{j^0corr} \quad (1)$$

$$\%\ IE = \frac{j^0corr - jcorr}{j^0corr} \times 100 \quad (2)$$

j^0_{corr} and j_{corr} represents the corrosion current density (with and without the inhibitor respectively).

2.5 Surface Analysis (Optical)

To analyse the surface of the immersed test samples of copper, metallurgical optical microscopy was employed to closely examine its surface morphology at a 40x magnification. This technique allowed for detailed observation of any changes, such as corrosion patterns, pitting, or deposits, that occurred on the copper surface after exposure to the test environment

3. Results and Discussion

3.1 Response of Copper Samples to Tilapia Fish Scale-Derived Hydroxyapatite

The electrochemical evaluation of copper corrosion in 1M HCl, using hydroxyapatite from Tilapia fish scales as a corrosion inhibitor was done through open circuit potential (OCP) analysis, Tafel polarization tests, and linear sweep voltammetry (LSV) measurements. Figures 1, 2, and 3 demonstrate that copper has more negative potentials and high corrosion in the acidic environment without the inhibitor (Ubogu *et al.,* 2024). At 30°C, the control samples had a corrosion potential (E_{corr}) of -0.625 V; at 40°C, -0.364 V; and at 50°C, -0.841 V, showing the most negative readings. Adding the inhibitor shifted potentials towards less negative values. At 50°C, 0.6 g of inhibitor resulted in -0.423 V, indicating better surface passivation as per Jmiai *et al.* (2021). This change proves that hydroxyapatite adsorbed well onto the copper substrate, forming a protective layer that suppressed the dissolution of the metal.

Corresponding author's email address: ojosundayfayomi3@gmail.com, osfayomi@bellsuniversity.edu.ng

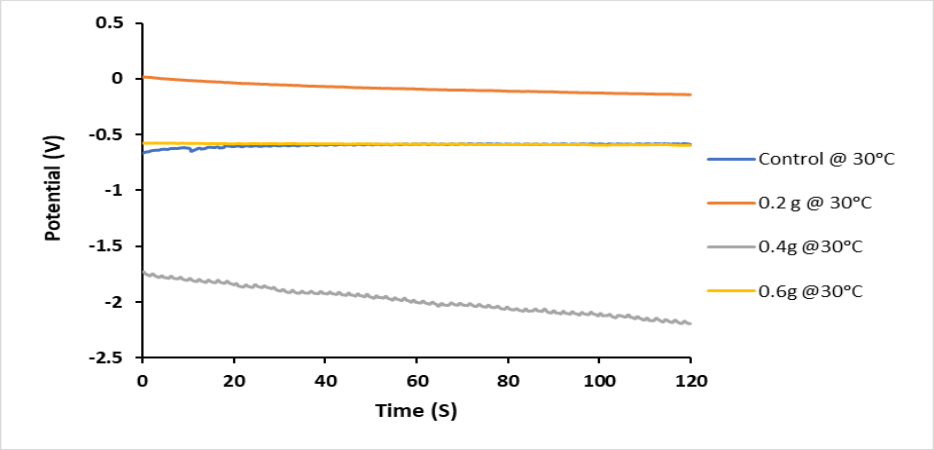

Figure 1: OCP Plot of the inhibited Copper sample at 30°C

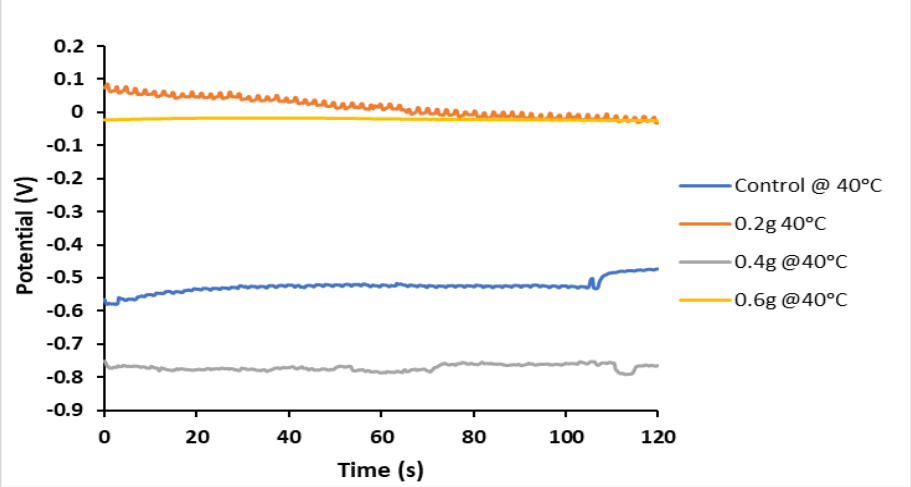

Figure 2: OCP Plot of the inhibited Copper sample at 40°C

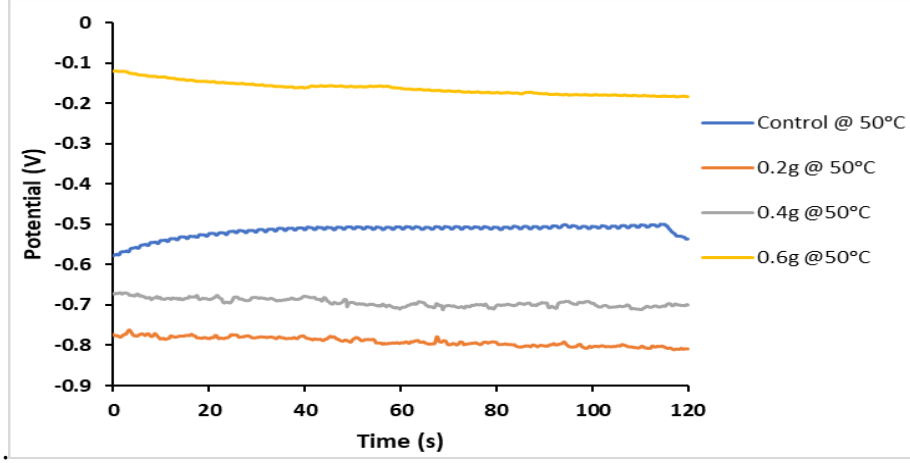

Figure 3: OCP Plot of the inhibited Copper sample at 50°C

Analysis of Tafel polarization data in Table 3 shows the effectiveness of the corrosion inhibitor, as reflected by a considerable decrease in corrosion current density (J_{corr}) with the addition of the inhibitor (Al-Amiery *et al.*, 2023). At 30°C, J_{corr} went down from 1.94E-04 A/cm² (control) to 2.82E-05 A/cm² (0.6 g), reflecting a significant drop in the corrosion rate from 2.27 mm/yr to 0.33 mm/yr. A similar trend was seen at 40°C, where J_{corr} dropped from 4.55E-04 A/cm² (control) to 5.82E-05 A/cm² (0.6 g), reflecting a reduction from 5.34 mm/yr to 0.68 mm/yr in the corrosion rate. At 50°C, the control sample recorded the highest J_{corr} at 5.13E-04 A/cm²; however, the addition of the inhibitor at 0.6 g lowered this reading to 3.14E-05 A/cm², thus reflecting a drop in the rate of corrosion from 6.02 mm/yr to 0.37 mm/yr. These decrease and an increase in polarization resistance (PR), which reached 922 Ω at 30°C and 829 Ω at 50°C for the 0.6 g dose, support the ability of the inhibitor to enhance corrosion resistance. The control samples exhibited the

Corresponding author's email address: ojosundayfayomi3@gmail.com, osfayomi@bellsuniversity.edu.ng

highest current densities across all temperatures, while the 0.6 g samples showed suppressed currents, confirming reduced copper oxidation and hydrogen evolution. This aligns with Zor *et al.* (2011), where increasing concentrations of amides reduced I_{corr} by over 90% in 1.0 M HCl, attributed to mixed-type inhibition via adsorption. The observed rise in polarization resistance (Rp) from 512 to 3,606 Ω·cm² further corroborates the formation of a protective inhibitor layer, mirroring the behavior of Tilapia HAp in this study. The study finds that control samples have the highest current densities across all temperatures. The trend in potential shifts, reduced J_{corr}, and increased PR suggests that Tilapia fish scale-derived hydroxyapatite reacts as a mixed-type inhibitor which would mean it affects both the anodic metal dissolution and cathodic hydrogen evolution (Marinescu, 2019).

Table 3: Tafel Data of the Experiments at 30°C, 40°C, and 50°C.

30°C				
Samples	E_{corr} (V)	J_{corr} (A/Cm^2)	CR (mm/yr)	PR (Ω
Control	-0.625	1.94E-04	2.27	1.34E+02
0.2 g	-0.517	1.45E-04	1.71	1.79E+02
0.4g	-1.653	7.74E-05	0.91	3.36E+02
0.6g	-0.700	2.82E-05	0.33	9.22E+02
40°C				
Control	-0.364	4.55E-04	5.34	5.71E+01
0.2g	-0.430	3.05E-04	3.58	8.51E+01
0.4g	-0.920	2.41E-04	2.82	1.08E+02
0.6g	-0.186	5.82E-05	0.68	4.47E+02
50°C				
Control	-0.841	5.13E-04	6.02	5.07E+01
0.2g	-0.872	4.62E-04	5.42	5.63E+01
0.4g	-0.813	2.14E-04	2.52	1.21E+02
0.6g	-0.423	3.14E-05	0.37	8.29E+02

Figures 4–6 present the LSV profiles for copper in 1M HCl at 30°C, 40°C, and 50°C. In the absence of HAp (Figure 4, control at 30°C), the anodic branch shows a sharp rise in current density beyond -0.5 V, corresponding to rapid copper dissolution. The cathodic branch similarly reflects vigorous hydrogen evolution. With 0.6 g HAp, both anodic and cathodic currents are suppressed by over an order of magnitude drops from, confirming the inhibitor's mixed-type behavior. At 40°C (Figure 5), the control sample exhibits even higher, but the 0.6 g HAp reduces this to, maintaining strong inhibition despite increased thermal agitation. By 50°C (Figure 6), the HAp's efficacy slightly diminishes, likely due to partial desorption of physically adsorbed HAp molecules. The LSV curves also reveal a widening passive region with higher HAp concentrations, implying enhanced surface coverage and delayed breakdown of the protective layer. The efficiency remained high at lower temperatures, though a slight decrease at 50°C suggests partial desorption of the inhibitor, which is common with physisorption mechanisms at elevated temperatures (Abdel-karim *et al.,* 2023).

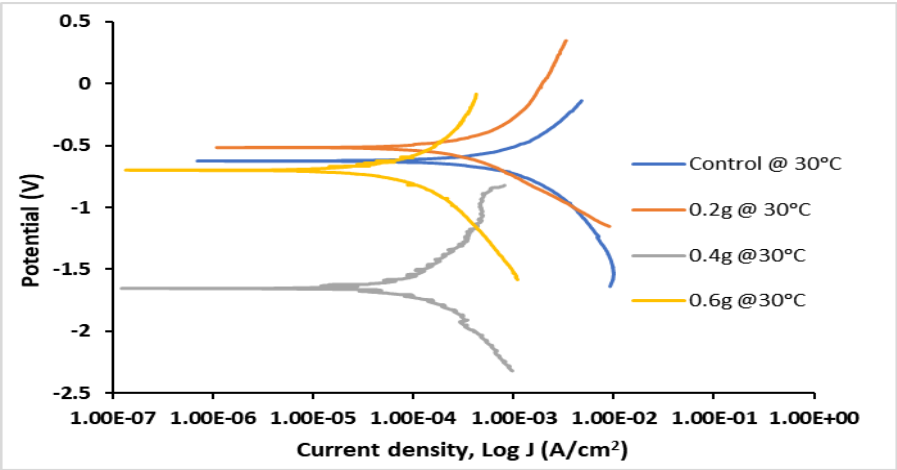

Figure 4: LSV Plot of the inhibited Copper sample at 30°C

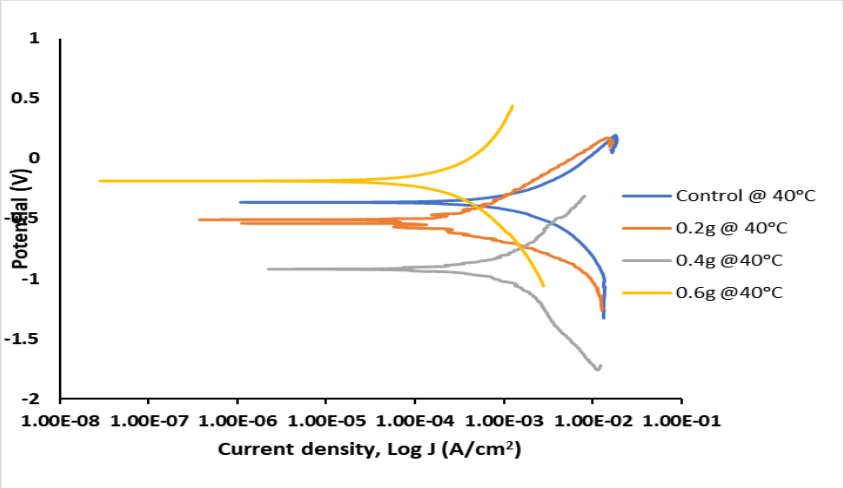

Figure 5: LSV Plot of the inhibited Copper sample at 40°C

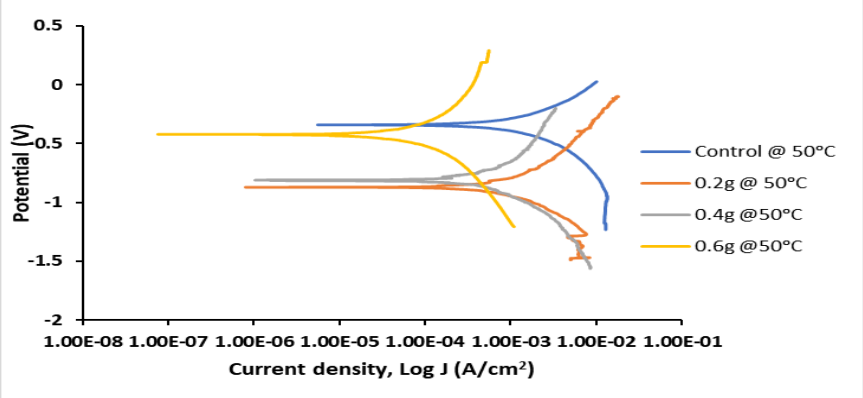

Figure 6: LSV Plot of the inhibited Copper sample at 50°C

3.2 Inhibitory Efficiency of Tilapia Fish-Scale-Derived Hydroxyapatite

The inhibition efficiency (IE) plot in Figure 7 of hydroxyapatite from tilapia fish scales showed an increase with different concentrations and temperatures. At 0.1 g concentration, the inhibition efficiency was relatively low, particularly at 50°C, indicating that the adsorption of the inhibitor on the copper sample decreases with increasing temperature. Conversely, at 0.2 g concentration, the IE showed a significant improvement, reaching about 60% at 30°C and 50% at 50°C. The maximum efficiency was at 0.3 g, where the IE was more than 85% at all tested temperatures, reaching a maximum of about 95% at 50°C, implying that the inhibitor acts best at higher concentrations. The trends in the corrosion rate (CR) plot of Figure 8 further support the inhibitory effects, with a decrease in CR being observed with an increase in the concentration of the inhibitor. The control samples showed the highest corrosion rates with values of 2.27 mm/year, 5.34 mm/year, and 6.02 mm/year at 30°C, 40°C, and 50°C, respectively, which reflect increased corrosion with increasing temperatures. However, the addition of 0.3 g of the inhibitor led to a significant decrease in CR to 0.33 mm/year at 30°C, 0.68 mm/year at 40°C, and 0.37 mm/year at 50°C, thus reflecting the protective nature of hydroxyapatite. The decrease in corrosion rate observed corresponds with an increase in polarization resistance (PR), thus supporting the hypothesis of inhibitor adsorption on the copper surface, which creates a barrier that reduces the corrosion rate, aligning with a study by Arukalam *et al.,* (2025) that investigated the inhibitive property of hydroxypropyl methylcellulose (HPC) on copper corrosion in 1.0 M HCl and 0.5 M H_2SO4 and the results showed that the corrosion rate decreased significantly in the presence of HPC, and the polarization resistance (PR) increased, indicating effective adsorption of the inhibitor on the copper surface and the formation of a protective barrier.

Corresponding author's email address: ojosundayfayomi3@gmail.com, osfayomi@bellsuniversity.edu.ng

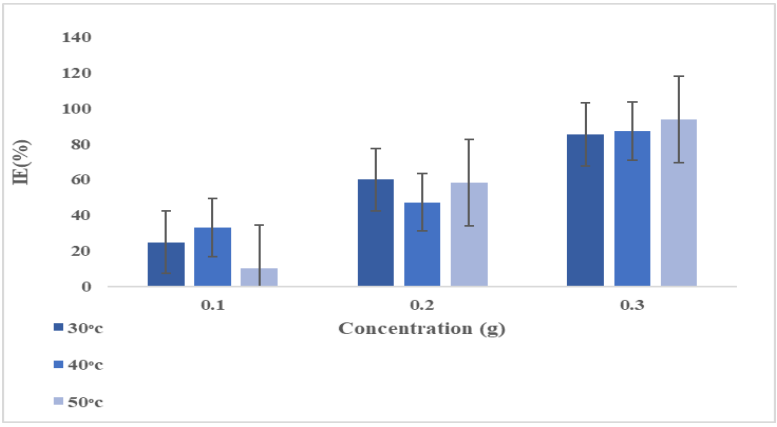

Figure 7: Inhibitor efficiency of Tilapia Fish Scale-Derived Hydroxyapatite

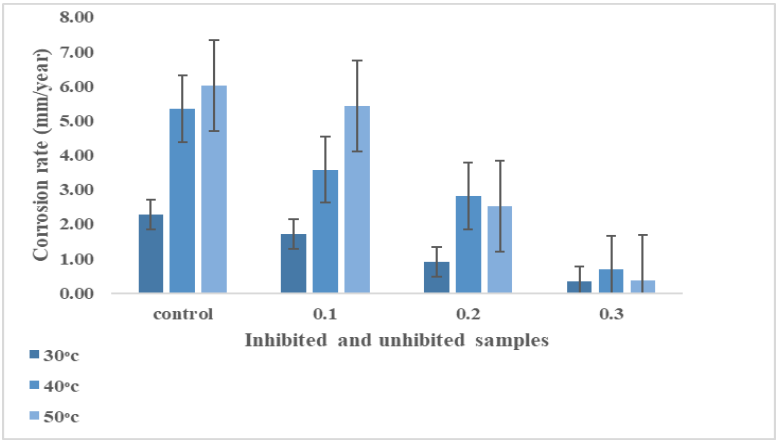

Figure 8: Corrosion Rate of The Copper Samples

3.3 Adsorption Response of Copper Samples

The Tilapia Fish Scale-Derived Hydroxyapatite adsorption behaviour on the copper surface in 1M HCl was analyzed using Langmuir, Freundlich, and Temkin isotherms. The Langmuir isotherm assumes monolayer adsorption on a homogeneous surface and its adsorption parameters in Table 4 gave low correlation coefficients- R^2=0.529, 0.108, and 0.777 at 30°C, 40°C, and 50°C, respectively, which indicates a poor fit. The adsorption equilibrium constant K_{ads} values of 1.197, 1.579, and 0.403 mol^{-1} suggest weaker adsorption at 50°C, implying that desorption occurs at elevated temperatures, reducing the inhibitor's effectiveness (Sharma *et al.,* 2019). The poor adherence to the Langmuir model suggests that adsorption is not strictly monolayer but involves interactions between adsorbed molecules and the surface. The Freundlich isotherm, which accounts for multilayer adsorption on different types of heterogeneous surfaces (Vigdorowitsch *et al.,* 2021), showed a high correlation as indicated by R^2 values in Table 4 of 0.991, 0.912, and 0.972 at temperatures of 30°C, 40°C, and 50°C, respectively. The rise in the adsorption constant K_{ads} from 1.602 to 3.159 mol^{-1} with increasing temperature shows that the extent of adsorption increases at higher temperatures. This is in agreement with the postulation that inhibitor molecules interact with different active sites on the copper surface, leading to a heterogeneous distribution (Vogler, 2013). The good fit with the Freundlich isotherm suggests that the phenomenon of adsorption goes beyond a single layer, involving multilayer adsorption, which increases efficacy at higher concentrations.

Table 4: Adsorption Parameters from Langmuir and Freundlich isotherm.

Temperature (°C)	$K_{ads}(mol^{-1})$	R^2
Langmuir Adsorption Isotherm		
30	1.196945161	0.529261967
40	1.579126492	0.108487207
50	0.40343823	0.776681035
Freundlich Adsorption Isotherm		
30	1.602157754	0.991497689
40	1.21075642	0.912338532
50	3.159289871	0.971582724

Corresponding author's email address: ojosundayfayomi3@gmail.com, osfayomi@bellsuniversity.edu.ng

The Temkin isotherm shown in Table 5 provided high correlation coefficients (R^2 = 0.997, 0.835, and 0.9960), validating the presence of lateral interactions among adsorbed molecules, correlating with a study by Chiter et al (2021). The free energy of adsorption (ΔG_{ads}) values of -15.27, -16.22, and -15.42 kJ/mol indicate a spontaneous adsorption process dominated by physisorption, as the values fall within the range of physical adsorption (<−20 kJ/mol) just as in a study by Husaini, (2021) that investigates the effect of benzaldehyde on aluminium corrosion inhibition in a solution of sulfuric acid. The experimental values of Gibbs free energy (ΔG_{ads}) were between -17.94 to -18.27 kJ/mol, indicating a spontaneous adsorption process dominated by physisorption. The increasing adsorption constant K_{ads} up to 40°C suggests an optimal adsorption temperature, while a slight decline at 50°C implies a minor desorption effect. The adsorption behavior of Tilapia fish scale-derived hydroxyapatite (HAp) on copper in 1M HCl was further analyzed using the Temkin isotherm, which accounts for interactions between adsorbed molecules and heterogeneous surface sites. Figure 9 plots surface coverage (θ) against the natural logarithm of inhibitor concentration (ln C) at 30°C, 40°C, and 50°C. The linear relationships (R^2 = 0.996–0.997) validate the Temkin model, with slopes (B) of 0.5485, 0.4632, and 0.7562 at 30°C, 40°C, and 50°C, respectively. Based on the findings obtained, Tilapia Fish Scale-Derived Hydroxyapatite acts as a mixed-type inhibitor that affects the anodic and cathodic processes related to copper corrosion.

Table 5: Adsorption Parameters from Temkin Adsorption isotherm.

Temperature (°C)	K_{ads}(mol^{-1})	ΔG_{ads} (KJmol^{-1})	R^2	ln(K_{ads})	1/T	ΔG_{ads}/T	B= Slope
30	7.7332	-15.2736	0.9966	2.0455	0.0033	-0.0504	0.5485
40	9.1793	-16.2238	0.8351	2.2169	0.0032	-0.0518	0.4632
50	5.6188	-15.4238	0.9958	1.7261	0.0031	-0.0478	0.7562

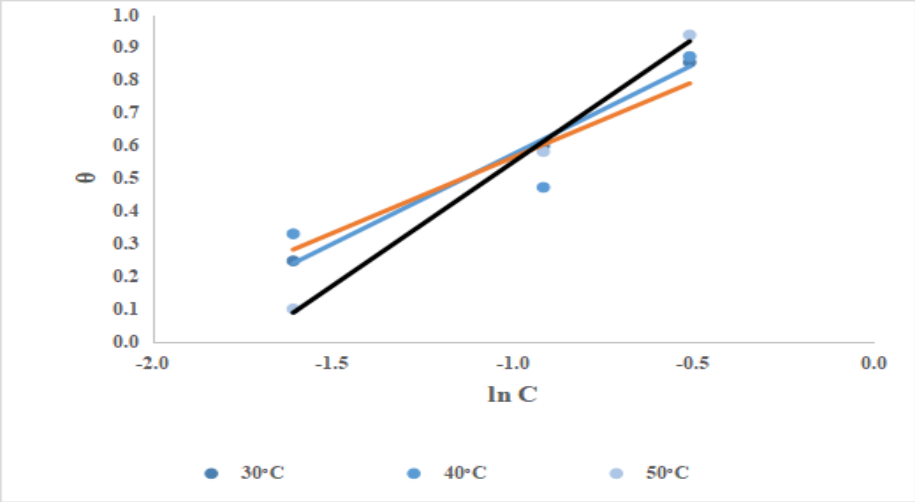

Figure 9: A graph of Θ against ln C.

The adsorption is predominantly physical, as confirmed by the ΔG_{ads} values and better fit to the Freundlich and Temkin models. The increase in adsorption with temperature suggests that molecular interactions and surface coverage enhance inhibition efficiency, making the extract more effective at higher concentrations. The HAp inhibitor forms a protective multilayer film-like cover on the surface of the copper, preventing direct acid attack and reducing corrosion rates effectively.

3.4 Optical Micrographs of the Test Copper Samples

Optical micrographs of the test samples exposed to corrosive environments, both with and without the addition of Hydroxyapatite as a corrosion inhibitor, are shown in Plate 1(a-d) at 40x magnification. Without the particulate inhibitor (Plate 1a), the copper samples indicate corrosion disturbance indicative of high corrosive activity. On the other hand, Plate 1(b-c) show that the surface morphology shows minimal evidence of corrosion in samples treated with different additional concentrations of the Hydroxyapatite inhibitor. Plate 1(d) has similar surface features; however, slight pitting is observed on the surface of the sample that has the highest particle concentration. These microscopic findings align with the findings obtained from electrochemical measurements.

Corresponding author's email address: ojosundayfayomi3@gmail.com, osfayomi@bellsuniversity.edu.ng

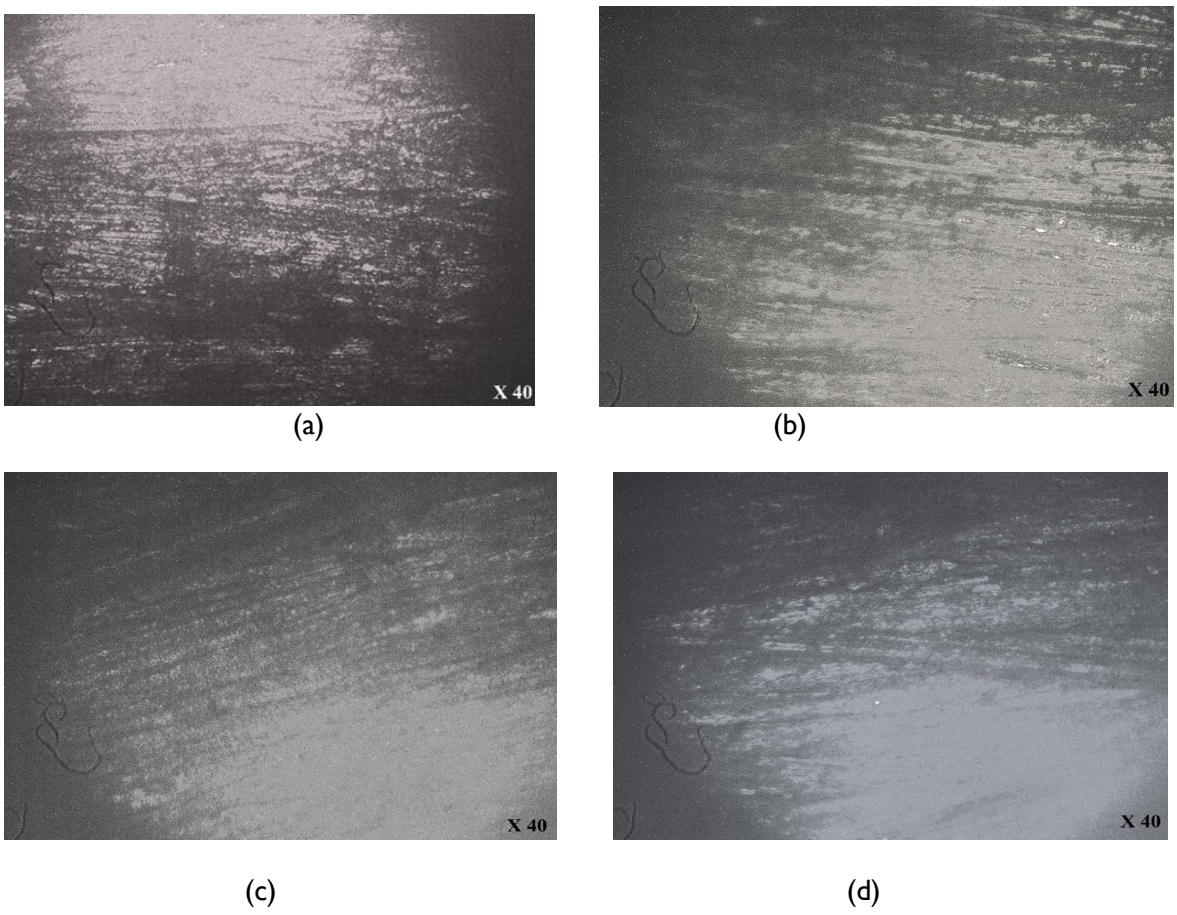

(a) (b)

(c) (d)

Plate 1 (a-d): Optical Micrographs of the Test Copper Samples (control, 0.2g, 0.4g, 0.6g).

3.5 Empirical Optimization

The inhibition efficiency (IE) from the DOE data in Table 6 of hydroxyapatite from Tilapia fish scales (TFS-HAp) was found to increase in effectiveness as the concentrations increased. At temperatures of 30°C, 40°C, and 50°C, the inhibitor performance was directly related to the increase in temperature, indicating increased surface coverage and probable chemical interaction between the inhibitor and copper. The corrosion rate (CR) analysis showed a significant reduction from 6.02 mm/year without the inhibitor to 0.37 mm/year at 50°C with 0.6 g of the inhibitor, thus proving the efficiency of TFS-HAp as a corrosion inhibitor. Likewise, at 40°C, CR reduced from 5.34 mm/year to 0.68 mm/year, and at 30°C, it reduced from 2.27 mm/year to 0.33 mm/year. These data suggest that the inhibitor performs best under conditions of increased concentrations and increased temperatures.

Table 6:Design of Experiment (DOE) Data

Factor A: Temperature (°c)	Factor B: Concentration (g)	Response 1: CR (mm/yr)
0	30	2.27
0.2	30	1.71
0.4	30	0.91
0.6	30	0.33
0	40	5.34
0.2	40	3.58
0.4	40	2.82
0.6	40	0.68
0	50	6.02
0.2	50	5.42
0.4	50	2.52
0.6	50	0.37

The findings from the ANOVA analysis in Table 7 further supports the statistical significance of the inhibition process, as indicated by a model F-value of 46.30 and a p-value that os lower than 0.0001, reflecting a strong

Corresponding author's email address: ojosundayfayomi3@gmail.com, osfayomi@bellsuniversity.edu.ng

relationship between concentration, temperature, and corrosion inhibition. Factor A (concentration) had the most significant effect (F = 147.12, p < 0.0001), thus confirming that the inhibitor dosage is critical for effective corrosion control. Factor B (temperature) also reflected a significant influence (F = 53.92, p = 0.0003), emphasizing the effect of temperature variations on the adsorption properties and effectiveness of the inhibitor. The interaction term (AB) also reflected statistical significance (F = 22.74, p = 0.0031), suggesting a synergistic effect between concentration and temperature. The model reliability was supported by a high R^2 value of 97.24%, in addition to an adjusted R^2 of 95.37% and a predicted R^2 of 87.70%, collectively reflecting that the model is a good representation of the experimental data. Furthermore, the coefficient of variation (CV%) of 16.46% further supports the validity of the findings. To enhance the effectiveness of the inhibitor, a central composite design (CCD) method was employed resulting in the development of a quadratic regression model that best predicts the relationship between concentration and temperature on the corrosion rate, as expressed in Equation 3. Upon optimization, it was established that the optimal inhibitor concentration is 0.471 g, coupled with a suitable temperature of 46.54°C, yielding a CR of 2.105 mm/year. The Fisher test was carried out to analyse the statistical validity of the model by way of comparing the mean square values from the model and the residual mean squares which confirms the sensitivity and reproducibility of the model, as shown in Figure 10.

$$\mathrm{CR} = 3.31 - 2.06\mathrm{A} + 1.14\mathrm{B} - 0.9922\mathrm{AB} - 0.3656A^2 - 0.6612B^2 \quad (3)$$

Table 7: ANOVA results showing copper-optimised response to Tilapia Fish Scale-Derived Hydroxyapatite Inhibition

Source	SS	DF	MS	F-value	p-value	Remark
Model	44.540	5.000	8.910	46.300	0.000	sig
A-Conc.	28.300	1.0000	28.3	147.12	< 0.0001	
B-Temp.	10.370	1.0000	10.37	53.92	0.0003	
AB	4.380	1.0000	4.38	22.74	0.0031	
A^2	0.317	1.0000	0.3169	1.65	0.2467	
B^2	1.170	1.0000	1.17	6.06	0.049	
Residual	1.150	6.0000	0.1924			
Cor Total	45.690	11.0000				

R^2 = 97.24%; Adjusted **R^2 =** 95.37%; predicted **R^2 =** 87.70%; CV%= 16.46

** SS- Sum of square; DF- Degree of Freedom; MS- Mean square; Sig.- Significant**

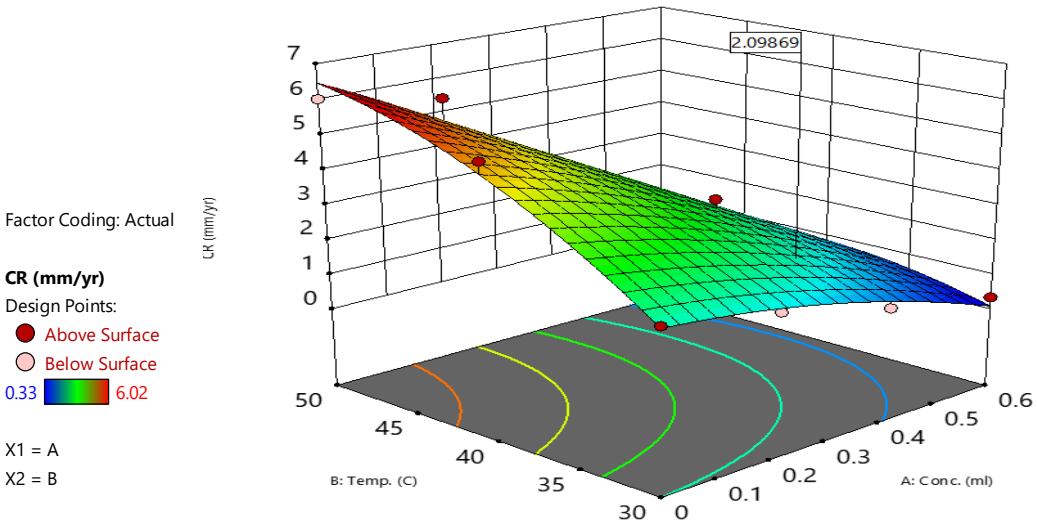

Figure 10: Tilapia Fish Scale-Derived Hydroxyapatite Inhibition Correlation with Temperature and Concentration

4. Conclusion

Tilapia fish scales, often discarded as waste, contain hydroxyapatite, a biocompatible material with potential applications in corrosion inhibition. This study evaluates hydroxyapatite extracted from fish scales as a green alternative to synthetic corrosion inhibitors for copper in acidic environments. The hydroxyapatite was obtained through a series of chemical and thermal treatments and then tested for its inhibition performance

Corresponding author's email address: ojosundayfayomi3@gmail.com, osfayomi@bellsuniversity.edu.ng

in 1M HCl. Electrochemical results showed that increasing the hydroxyapatite concentration significantly reduced the corrosion rate, with a maximum inhibition efficiency of 95% at 0.6 g. The inhibitor formed a stable multilayer protective film on the copper surface, preventing metal dissolution. Adsorption studies confirmed a strong adherence of the inhibitor molecules to the metal surface, with the Freundlich and Temkin models best describing the adsorption behavior. Microscopic analysis further validated the protective effect, showing reduced surface roughness and fewer corrosion pits in treated samples. Statistical optimization identified 0.471 g of hydroxyapatite at 46.54°C as the optimal conditions for maximum inhibition. These findings highlight the potential of fish scale-derived hydroxyapatite as a sustainable and effective corrosion inhibitor, addressing both environmental concerns and industrial corrosion challenges.

Acknowledgements

Bells University of Technology is gratefully acknowledged for its support during the research study.

References

Abdel-karim, AM., Ahmed, YM. and El-Masry, MM. 2023. Ag-CuO/epoxy hybrid nanocomposites as anti-corrosive coating and self-cleaning on copper substrate. Scientific Reports 13(1): 19248–19251.

Abdullah, NH., Mohamed Noor, AA., Mat-Rasat, MS., Mamat, S., Mohamed, M., Mohd Shohaimi, NA. and Mohd Amin, MF. 2020. Preparation and characterization of calcium hydroxyphosphate (hydroxyapatite) from tilapia fish bones and scales via calcination method. Materials Science Forum 1010(1): 596–601.

Abod, BM., Al-Alawy, RM., Khadom, AA. and Kamar, FH. 2019. Experimental and theoretical studies for tobacco leaf extract as an eco-friendly inhibitor for steel in saline water. Journal of Bio- and Tribo-Corrosion 5(3): 75–78.

Al-Amiery, A., Isahak, WNRW. and Al-Azzawi, WK. 2023. Multi-method evaluation of a 2-(1,3,4-thiadiazole-2-yl) pyrrolidine corrosion inhibitor for mild steel in HCl. Scientific Reports 13(1): 9770–9773.

Arthur, DE., Jonathan, A., Ameh, PO. and Anya, C. 2013. A review on the assessment of polymeric materials used as corrosion inhibitor of metals and alloys. International Journal of Industrial Chemistry 4(1): 1–4.

Arukalam, IO., Uzochukwu, IN., Uche, R., Udunwa, DI., Egole, CP. and Ndukwe, AI. 2025. Inhibitive property of hydroxypropyl methylcellulose on acid corrosion of copper: Experimental and computational simulation. Bulletin of Materials Science 48(1): 40–43.

Aydinsoy, EA., Aghamaliyev, ZZ., Aghamaliyeva, DB. and Abbasov, VB. 2024. A systematic review of corrosion inhibitors in marine environments: Insights from the last 5 years. Processing of Petrochemistry and Oil Refining 25(3): 1–4.

Chinh, NT., Manh, VQ., Trung, VQ., Lam, TD., Huynh, MD., Tung, NQ. and Hoang, T. 2019. Characterization of collagen derived from tropical freshwater carp fish scale wastes and its amino acid sequence. Natural Product Communications 14(7): 1–4.

Chiter, F., Costa, D., Maurice, V. and Marcus, P. 2021. Corrosion inhibition of locally de-passivated surfaces: DFT study of 2-mercaptobenzothiazole on copper. NPJ Materials Degradation 5(1): 52–55.

Coppola, D., Lauritano, C., Palma Esposito, F., Riccio, G., Rizzo, C. and de Pascale, D. 2021. Fish waste: From problem to valuable resource. Marine Drugs 19(2): 116–119.

DileepKumar, VG., et al. 2022. A review on the synthesis and properties of hydroxyapatite for biomedical applications. Journal of Biomaterials Science, Polymer Edition 33(2): 229–232.

Duan, R., Ying, L. and Zhang, Y. 2004. Monitoring the decalcifying process of fish scale by titration. Journal of Huaihai Institute of Technology (Natural Science Edition) 13(1): 54–57.

Ezzat, A., Motaal, SMA., Ahmed, AS., Sallam, HB., El-Hossiany, A. and Fouda, A. 2022. Corrosion inhibition of carbon steel in 2.0 M HCl solution using novel extract (Pulicaria undulata). Biointerface Research in Applied Chemistry 12(5): 6415–6418.

Corresponding author's email address: ojosundayfayomi3@gmail.com, osfayomi@bellsuniversity.edu.ng

Husaini, M. 2021. Corrosion inhibition effect of benzaldehyde (methoxybenzene) for aluminium in sulphuric acid solution. Algerian Journal of Engineering and Technology 4(1): 74–77.

Jmiai, A., Tara, A., El Issami, S., Hilali, M., Jbara, O. and Bazzi, L. 2021. A new trend in corrosion protection of copper in acidic medium using Jujube shell extract: Experimental, quantum chemistry and Monte Carlo study. Journal of Molecular Liquids 322(1): 114509–114512.

Kadhim, A., Al-Amiery, AA., Alazawi, R., Al-Ghezi, MKS. and Abass, RH. 2021. Corrosion inhibitors: A review. International Journal of Corrosion and Scale Inhibition 10(1): 54–57.

Kehinde, EI., Fayomi, OS. and Atiba, JO. 2025. Corrosion behaviour of AA6063 alloy in acidic chloride conditions: Inhibition by Pennisetum glaucum extract. Journal of Bio- and Tribo-Corrosion 11(2): 1–4.

Li, H., Zhang, S. and Qiang, Y. 2021. Corrosion retardation effect of a green cauliflower extract on copper in H_2SO_4 solution: Electrochemical and theoretical explorations. Journal of Molecular Liquids 321(1): 114–117.

Marinescu, M. 2019. Recent advances in the use of benzimidazoles as corrosion inhibitors. BMC Chemistry 13(1): 136–139.

Nyambi, NF., Premlall, K. and Govender, KK. 2024. The physicochemical characterisation and computational studies of tilapia fish scales as a green inhibitor for steel corrosion. Engineering Proceedings 67(1): 1–4.

Panda, NN., Pramanik, K. and Sukla, LB. 2014. Extraction and characterization of biocompatible hydroxyapatite from freshwater fish scales for tissue engineering scaffold. Bioprocess and Biosystems Engineering 37(1): 433–436.

Selimin, MA., Latif, AFA., Lee, CW., Muhamad, MS., Basri, H. and Lee, TC. 2022. Adsorption efficiency of hydroxyapatite synthesised from black tilapia fish scales for chromium (VI) removal. Materials Today: Proceedings 57(1): 1142–1145.

Sharma, S., Ko, X., Kurapati, Y., Singh, H. and Nešić, S. 2019. Adsorption behavior of organic corrosion inhibitors on metal surfaces: Some new insights from molecular simulations. Corrosion 75(1): 90–93.

Sockalingam, K. and Abdullah, HZ. 2015. Extraction and characterization of gelatin biopolymer from black tilapia (Oreochromis mossambicus) scales. AIP Conference Proceedings 1669(1): 101–104.

Tacon, AG. 2020. Trends in global aquaculture and aquafeed production: 2000–2017. Reviews in Fisheries Science & Aquaculture 28(1): 43–46.

Ubogu, AE., Fayomi, OS. and Atiba, JO. 2024. Microstructural and anti-corrosion responses of copper in NaCl-fishbone ash environment. 2024 IEEE 5th International Conference on Electro-Computing Technologies for Humanity (NIGERCON) 1(1): 1–4.

Vigdorowitsch, M., Pchelintsev, A., Tsygankova, L. and Tanygina, E. 2021. Freundlich isotherm: An adsorption model complete framework. Applied Sciences 11(17): 8078–8081.

Vogler, EA. 2013. Surface modification for biocompatibility. In: Lakhtakia, A., & Martín-Palma, RJ. (Eds.), Engineered Biomimicry. Boston: Elsevier, 189–192.

Wang, H., Wang, X., Wang, H., Wang, L. and Liu, A. 2007. DFT study of new bipyrazole derivatives and their potential activity as corrosion inhibitors. Journal of Molecular Modeling 13(1): 147–150.

Zainol, I., Adenan, NH., Rahim, NA. and Jaafar, CNA. 2019. Extraction of natural hydroxyapatite from tilapia fish scales using alkaline treatment. Materials Today: Proceedings 16(1): 1942–1945.

Zhao, Z., Sun, M., Xia, J., Xu, H. and Wu, Y. 2025. A specific calcium silicate hydrate (PC/SP/CA-H) for simultaneous removal of phosphate and fluoride from low concentration water: Feasible and mechanisms research. Journal of Water Process Engineering 71(1): 107312–107315.

Zor, S., Saracoglu, M., Kandemirli, F. and Arslan, T. 2011. Inhibition effects of amides on the corrosion of copper in 1.0 M HCl: Theoretical and experimental studies. Corrosion Journal of Science and Engineering 67(12): 125001–125004.

Corresponding author's email address: ojosundayfayomi3@gmail.com, osfayomi@bellsuniversity.edu.ng